

## Article

# Dynamic Optimal Power Dispatch in Unbalanced Distribution Networks with Single-Phase Solar PV Units and BESS

Jordan Radosavljević <sup>1</sup>, Aphrodite Ktena <sup>2,\*</sup>, Milena Gajić <sup>3</sup>, Miloš Milovanović <sup>1</sup> and Jovana Živić <sup>1</sup>

<sup>1</sup> Faculty of Technical Sciences, University of Priština in Kosovska Mitrovica, 38220 Kosovska Mitrovica, Serbia; jordan.radosavljevic@pr.ac.rs (J.R.)

<sup>2</sup> General Department, National and Kapodistrian University of Athens, Evripos Campus, 34400 Evia, Greece

<sup>3</sup> Technical Faculty in Bor, University of Belgrade, 19210 Bor, Serbia; mgajic@tfbor.bg.ac.rs

\* Correspondence: apktena@uoa.gr

**Abstract:** Battery energy storage systems (BESSs) are a promising solution for increasing efficiency and flexibility of distribution networks (DNs) with a significant penetration level of photovoltaic (PV) systems. There are various issues related to the optimal operation of DN with integrated PV systems and BESS that need to be addressed to maximize DN performance. This paper deals with day-ahead optimal active–reactive power dispatching in unbalanced DN with integrated single-phase PV generation and BESS. The objectives are the minimization of cost for electricity, energy losses in the DN, and voltage unbalance at three-phase load buses by optimal management of active and reactive power flows. To solve this highly constrained non-linear optimization problem, a hybrid particle swarm optimization with sigmoid-based acceleration coefficients (PSOS) and a chaotic gravitational search algorithm (CGSA) called the PSOS-CGSA algorithm is proposed. A scenario-based approach encompassing the Monte Carlo simulation (MCS) method with a simultaneous backward reduction algorithm is used for the probabilistic assessment of the uncertainty of PV generation and power of loads. The effectiveness of the proposed procedure is evaluated through a series of test cases in a modified IEEE 13-bus feeder. The simulation results show that the proposed approach enables a large reduction in daily costs for electricity, as well as a reduction in expected daily energy losses in the DN by 22% compared to the base case without BESS while ensuring that the phase voltage unbalance rate (PVUR) is below the maximum limit of 2% for all three-phase buses in the DN.

**Keywords:** distribution network; PV generation; battery energy storage; optimal power dispatch; uncertainty; scenario reduction



**Citation:** Radosavljević, J.; Ktena, A.; Gajić, M.; Milovanović, M.; Živić, J. Dynamic Optimal Power Dispatch in Unbalanced Distribution Networks with Single-Phase Solar PV Units and BESS. *Energies* **2023**, *16*, 4356. <https://doi.org/10.3390/en16114356>

Academic Editor: Alon Kuperman

Received: 19 April 2023

Revised: 18 May 2023

Accepted: 23 May 2023

Published: 26 May 2023



**Copyright:** © 2023 by the authors. Licensee MDPI, Basel, Switzerland. This article is an open access article distributed under the terms and conditions of the Creative Commons Attribution (CC BY) license (<https://creativecommons.org/licenses/by/4.0/>).

## 1. Introduction

In light of the recent energy crisis, in the midst of the energy transition towards carbon-free power systems, the advantages of renewable energy sources (RESs), such as photovoltaic (PV) generators, the growth of which has been exponential over the last twenty years [1], position them in the center of related policies. However, they suffer from variability and stochasticity of output power, which is their main drawback [2] and a challenge in terms of attracting the interest of the research community. A promising approach towards a more flexible use of PV sources is their combination with battery energy storage systems (BESSs) to fully exploit the potential of PV units integrated into distribution networks (DNs) [3,4].

In the last few years, a number of authors have addressed the issues of optimal power dispatch in DN with integrated BESSs. These studies have been focused on several main aspects, such as modeling BESSs; defining the BESS function in DN, i.e., objective functions of the optimization problem; defining control variables, dependent variables, and technical constraints; and the choice of solution methods.

A BESS is a combination of a voltage source converter and a battery pack such that the active and reactive power can be controlled independently [5–10]. In most research articles,

BESSs are modeled as a set of equations defining that the stored energy at any given time segment is a function of the stored energy and the charge/discharge power at the previous time segment. Internal losses of BESSs are accounted for through the charge/discharge efficiency coefficients or functions. The limits of the reactive power output to be provided by a BESS are also defined in these models.

Depending on the function that a BESS performs in the DN, the objectives for the optimal power dispatch can be summarized in three groups: technical objectives, financial objectives, and multi-objectives. Financial objectives can be related to the maximization of revenues of an RES-BESS based on hybrid power plant [11]; the reduction in the energy cost from the source grid [12,13]; or the minimization of distributed generator dispatch costs [14], power generation costs, and load-shedding costs [6]. Technical objectives are the base objectives and include static voltage stability improvement [7], transient voltage stability enhancement [9], energy loss minimization [10], voltage fluctuation mitigation [15], minimization of the voltage deviations at load buses [16], and reduction in power imbalances [17]. Researchers often adopt multi-objective functions with different combinations of financial and technical objectives, such as the simultaneous maximization of the total yield from an RES and minimization of the total costs of the energy loss in DNs [5] or the simultaneous minimization of power exchange cost between a DN and the transmission network and the penalty cost of the voltage deviation in the DN [8].

In its most general mathematical formulation, the optimal power dispatch in DNs with integrated RES and BESS is a non-linear, non-convex, large-scale, dynamic optimization problem with constraints. There are two approaches to solving it, namely classical optimization methods and metaheuristic methods.

Non-linear optimization models are implemented in the GAMS environment and solved using CONOPT3 solver [5], CPLEX solver [6], and KNITRO solver [12]. The big  $M$  method was used in [8] to transform the model into a mixed-integer linear programming problem and solved using commercial software. The interior-point solver *fmincon* in MATLAB R2021a [10] and the simplex solver through the *docplex* Python library [11] are also suggested for optimal power flow in DNs with a BESS, whereas Giuntoli et al. [14] used the CaADdi framework to interface with the IPOPT solver for non-linear programming. In recent research, some population-based methods, such as PSO, have been proposed to find the optimal power dispatch solution in DNs with BESSs [7,16].

The focus of this paper, which is a continuation of the research started in [13], is the problem of optimal power dispatch in unbalanced DNs with single-phase PV generation and BESSs. The main contributions of this study are as follows:

1. A dynamic model of the optimal active power dispatch (OAPD) in unbalanced DNs with single-phase PV and BESSs is proposed to minimize energy costs from the source network;
2. The optimal reactive power dispatch (ORPD) in unbalanced DNs with single-phase PV and BESSs is considered. The objective functions consist of minimizing energy losses and voltage unbalance at three-phase load buses with the reactive powers of solar PV inverters and BESSs as control variables;
3. A scenario-based approach encompassing the MSC method and the simultaneous backward reduction technique is proposed for modeling the uncertainty of PV generation and load in DNs;
4. A novel hybrid PSOS-CGSA algorithm is proposed and applied to solve optimal active-reactive power dispatch problems;
5. A modified IEEE 13-bus feeder for evaluating the solvability and applicability of the proposed approach is proposed and defined.

The proposed methodology is presented in a structured way through the flowchart in Figure 1.

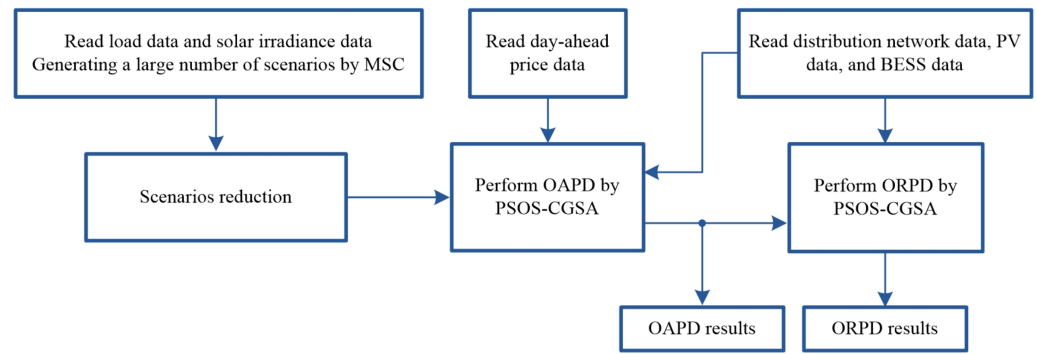


**Figure 1.** Flow chart of the proposed methodology.

The rest of this paper is organized as follows. In Section 2, a scenario-based model is formulated for the optimal dispatching of active power in DNs by operating mode control of BESSs. The problem of optimal reactive power dispatch in unbalanced DNs with single-phase PV and BESS inverters is elaborated in Section 3. The solution method based on the hybrid PSOS-CGSA metaheuristic algorithm is briefly presented in Section 4. The simulation results are discussed in Section 5, whereas the main conclusions are listed in Section 6.

## 2. Active Power Dispatch by BESS

The battery operation mode is determined by two basic parameters: charge/discharge power ( $P_{bat}$ ) and state of charge (SoC). Since the battery capacity is limited, the SoC of the battery must be viewed as a dynamic quantity, as follows [11]:

$$SoC_{\phi}(t) = SoC_{\phi}(t - \Delta t) + \Delta SoC_{\phi} \tag{1}$$

$$\Delta SoC_{\phi} = \left[ P_{bat,ch,\phi}(t - \Delta t)\eta_{ch,\phi} - \frac{P_{bat,dch,\phi}(t - \Delta t)}{\eta_{dch,\phi}} \right] \frac{\Delta t}{C_{bat,\phi}} \tag{2}$$

where  $C_{bat,\phi}$  is the total capacity of the battery;  $P_{bat,ch}$  and  $P_{bat,dch}$  are the charging and discharging power of the battery, respectively;  $\eta_{ch}$  and  $\eta_{dch}$  are the charging and discharging efficiency, respectively;  $\Delta t$  is the time segment (for example, 1 h); and  $\phi$  denotes the phase, where  $\phi \in (a,b,c)$ .

Battery power and SoC must always be within defined limits, as follows:

$$0 \leq P_{bat,ch,\phi}(t) \leq P_{bat,chmax} \tag{3}$$

$$0 \leq P_{bat,dch,\phi}(t) \leq P_{bat,dchmax} \tag{4}$$

$$SoC_{min} \leq SoC_{\phi}(t) \leq SoC_{max} \tag{5}$$

$$SoC_{\phi}(t = 0) = SoC_{\phi}(t = T) \tag{6}$$

$$P_{bat,ch,\phi}(t) \cdot P_{bat,dch,\phi}(t) = 0 \tag{7}$$

where  $P_{bat,chmax}$  and  $P_{bat,dchmax}$  are the maximum charging and discharging powers of the battery, respectively;  $SoC_{min}$  and  $SoC_{max}$  are the predefined minimum and maximum charge levels, respectively; and  $T$  is a time horizon, e.g., 24 h.

Battery charge/discharge power ( $P_{bat}$ ) and SoC are mutually dependent variables. Taking into account the variability of the electricity price, their relationship can be expressed as follows [13]:

$$P_{bat,\phi}(t) = \begin{cases} 0 & \text{if } c_g(t) \leq c_{gav} \\ & \text{and } SoC_\phi(t) = SoC_{max} \\ a_\phi(t) \cdot P_{bat,chmax} & \text{if } c_g(t) \leq c_{gav} \\ & \text{and } SoC_{min} \leq SoC_\phi(t) < SoC_{max} \\ 0 & \text{if } c_g(t) > c_{gav} \\ & \text{and } SoC_\phi(t) = SoC_{min} \\ -a_\phi(t) \cdot P_{bat,dchmax} & \text{if } c_g(t) > c_{gav} \\ & \text{and } SoC_{min} < SoC_\phi(t) \leq SoC_{max} \end{cases} \quad (8)$$

where  $c_g(t)$  is the day-ahead electricity price from the source grid at time  $t$ ,  $c_{gav}$  is the average electricity price during the day, and  $a_\phi(t)$  is a coefficient within the range [0–1].

The coefficient  $a_\phi(t)$ , which defines the power of the BESS, can be determined in different ways. In [13], the coefficient  $a_\phi(t)$  was calculated based on the relation of the electricity price at the time  $t$  with the mean electricity price during the day. A similar approach was adopted in [18], where the coefficient  $a_\phi(t)$  was calculated as a function of the difference in the electricity price from the predefined lower price limit for discharging and the upper price limit for charging. However, the charging/discharging powers of the BESS determined in this way do not guarantee the optimal dispatch of the active power according to the adopted objective function. Therefore, in this paper, the coefficient  $a_\phi(t)$  is considered as a control variable, the value of which is optimized to ensure the minimization of a given objective function.

The basic equation of the active power dispatch problem is the power balance constraint (9), which must be satisfied at each time segment ( $t$ ):

$$\sum_{\phi \in (a,b,c)} P_{g,\phi}(t) = \sum_{\phi \in (a,b,c)} [P_{L,\phi}(t) - P_{PV,\phi}(t) + P_{bat,\phi}(t)] \quad (9)$$

where  $P_{g,\phi}(t)$  is the active power from/to the source grid at time  $t$  in phase  $\phi$ ,  $P_{L,\phi}(t)$  is the total active power of the load at time  $t$  in phase  $\phi$ ,  $P_{PV,\phi}(t)$  is the total active power generation of PV units at time  $t$  in phase  $\phi$ , and  $P_{bat,\phi}(t)$  is the active power of the battery at time  $t$  in phase  $\phi$ , where  $\phi \in (a,b,c)$ .

### 2.1. Objective Function for OAPD

By controlling the operating mode of the battery, i.e., the charging/discharging power and SoC, the active power flows in the distribution network can be significantly influenced. In this way, the exchange power with the source power grid is directly affected, as well as other parameters of the distribution networks, such as power losses, voltage profile, etc. The operating costs of the distribution network mostly depend on the value of the energy from/to the source grid. Considering various PV generation and load demand scenarios with their probabilities, the objective function for OAPD can be formulated as the minimization of the expected cost for electricity, as follows:

$$\min Cost = \min \left[ \sum_{\xi=1}^{\Xi} (C_g^\xi + C_{bat}^\xi) p(\xi) \right] \quad (10)$$

$$C_g^\xi = \sum_{t=1}^T \sum_{\phi \in a,b,c} c_g(t) P_{g,\phi}^\xi(t) \quad (11)$$

$$C_{bat}^\xi = \sum_{t=1}^T \sum_{\phi \in a,b,c} c_{bat} P_{bat,\phi}^\xi(t) \quad (12)$$

where  $\xi$  and  $\Xi$  are the current scenario and the total number of scenarios, respectively;  $p(\xi)$  is the probability of scenario  $\xi$ ;  $C_g^\xi$  and  $C_{bat}^\xi$  are the total cost for electricity from the

source grid and operating cost of the battery in scenario  $\zeta$ , respectively;  $c_g$  and  $c_{bat}$  are the electricity price from the source grid and the unit operating cost of the battery, respectively; and  $T$  is the considered period (i.e., 24 h).

Two assumptions should be kept in mind here, namely:

- The retail electricity prices have the same daily profile as the wholesale electricity prices and fluctuate hourly;
- The DN transacts the wholesale markets through some energy agent such as an aggregator.

The power output of a PV source is determined by the solar irradiation at a given moment, and its value cannot be influenced. Therefore, the cost of PV generation is not taken into account in the objective function (10) because it cannot be optimized by controlling the charge/discharge power of the battery.

For stable operation, constraints (3)–(7) and (9) must be satisfied. The output power of the PV generator is limited by the maximum output power, i.e., the nominal power. Additionally,  $P_{g,\phi}(t)$  must be restricted by minimum and maximum values.

## 2.2. Modeling of Uncertainties

### 2.2.1. PV Generation Modeling

The power of the PV source as a function of solar irradiance can be expressed as follows [16]:

$$P_{PV}(S) = \begin{cases} P_{pvn} \frac{S^2}{S_{stc} R_c} & \text{for } S < R_c \\ P_{pvn} \frac{S}{S_{stc}} & \text{for } S \geq R_c \end{cases} \quad (13)$$

where  $P_{pvn}$  is the nominal power of the PV source,  $S$  is the solar irradiance on the PV module surface,  $S_{stc}$  is the solar irradiance under standard test conditions, and  $R_c$  is a certain irradiance point.

To model the stochastic nature of the solar irradiance, it is most convenient to use the Beta probability density function (PDF):

$$f_b(S) = \begin{cases} \frac{\Gamma(\alpha+\beta)}{\Gamma(\alpha)\Gamma(\beta)} S^{\alpha-1} (1-S)^{\beta-1}, & \text{for } 0 \leq S \leq 1, \alpha \geq 0, \beta \geq 0 \\ 0, & \text{otherwise} \end{cases} \quad (14)$$

where  $f_b(S)$  is the Beta function of the solar irradiance ( $S$ ),  $\alpha$  and  $\beta$  are the shape parameters of the Beta distribution, and  $\Gamma$  is the Gamma function.

Based on the data of the long-term measurement of the solar irradiance in a given area, characteristic daily diagrams of the solar radiation can be estimated with statistical indicators, i.e., mean value ( $\mu_S$ ) and standard deviation of the solar irradiance ( $\sigma_S$ ) in a given time interval  $t$  (e.g., an hour). Using the mean value and standard deviation of the solar irradiance, the shape parameters of the Beta PDF can be calculated for a time interval ( $t$ ) as follows:

$$\beta = (1 - \mu_S) \cdot \left( \frac{\mu_S(1 + \mu_S)}{(\sigma_S)^2} - 1 \right) \quad (15)$$

$$\alpha = \frac{\mu_S \cdot \beta}{1 - \mu_S} \quad (16)$$

### 2.2.2. Load Modeling

The normal (Gaussian) probability function is most commonly used to model load uncertainty in distribution systems. Generally, the load level is assumed to be a random variable ( $L$ ) following the same PDF within each hour of a given daily load diagram [2].

$$f_n(L) = \frac{1}{\sqrt{2\pi}\sigma_L} e^{-\frac{(L-\mu_L)^2}{2\sigma_L^2}} \quad (17)$$

$$L = \mu_L + \sqrt{2}\sigma_L \text{erf}^{-1}(2r - 1) \quad (18)$$

where  $\mu_L$  and  $\sigma_L$  are the mean value and standard deviation of  $L$ , respectively;  $r$  is a random number in the range of  $[0, 1]$ ; and  $\text{erf}(\cdot)$  and  $\text{erf}^{-1}(\cdot)$  are the error function and the inverse error function, respectively.

### 2.2.3. Scenario Generation

The Monte Carlo simulation (MCS) method is suitable for modeling the uncertainties of solar irradiance and load level. Starting from probability density functions for solar irradiance and load, the parameters of which are determined based on historical data, e.g., previous years, the MCS method can generate a large number of scenarios for day-ahead profiles of solar irradiance and load levels. Although a larger number of scenarios (e.g., several thousand) provides a more faithful modeling of the uncertainty of the output power of the PV source and the load level, on the other hand, it means a higher computation burden. In distribution network operation control applications, such as optimal power flow, methods with high accuracy and low computational burden are needed.

As a compromise between a good approximation (modeling) of the uncertainty of stochastic input variables (solar irradiance and load) on the one hand and a significant reduction in calculation time on the other hand, a scenario reduction strategy aggregating similar scenarios can be applied. In doing so, it must be ensured that the metric of the probability distribution of the reduced set is close enough to the original set of scenarios. There are several algorithms for reducing the number of scenarios, such as k-means clustering, backward reduction, and fast forward selection. In this work, the simultaneous backward reduction algorithm [19–21] was employed to reduce a ternary scenario tree for the daily PV generations and load profiles.

### 3. Optimal Reactive Power Dispatch

In this paper, it is assumed that PV arrays and batteries are connected to unbalanced DNs via single-phase converters. Depending on the nominal apparent power of the converter and the active power level of the corresponding PV source or battery, they have the ability to control the generation/absorption of reactive power, that is, they can be used as an additional regulation resource in DNs [13,22], as illustrated in Figure 2.

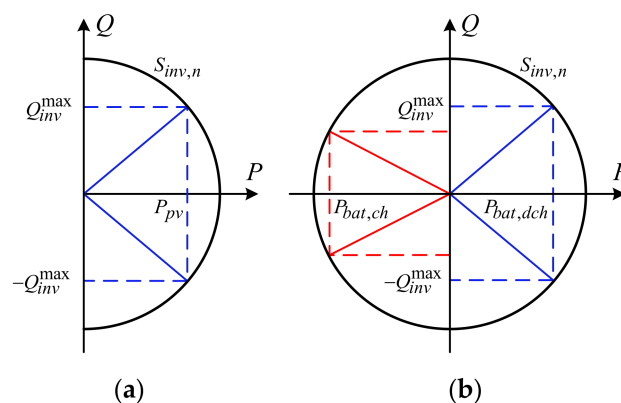


**Figure 2.** Inverter capability curve: (a) diagram of the two-quadrant regulating capacity of a PV model; (b) diagram of the four-quadrant regulating capacity of a BESS model. The red line indicates “consumer mode” and the blue line “generator mode” considering active power from/to the distribution network.

In this paper, we do not specifically deal with power converter topologies. For practical realization, several power converter topologies can be applied to connect BESSs to the grid [23]. The conventional structure of power converter for BESSs consists of a bidirectional DC/DC stage and a DC/AC stage. The basic requirement that they must fulfill for the

ORPD problem is that their rated power be equal to or greater than the rated power of the battery and that they have the ability to control the reactive power through a DC bus capacitor.

Therefore, for DNs with PV units and BESSs, the problem of ORPD can be posed as a problem of determining the optimal reference values of the available reactive powers of the inverters and the slack bus voltage magnitudes with a certain objective function under specified active power outputs of all PV and BESS inverters representing the solution of the active power dispatch, as explained in Section 2.

### 3.1. Objective Function for ORPD

#### 3.1.1. Active Power Loss Minimization

The level of active power losses is one of the most important indicators of the efficiency of distribution network management because they represent the direct costs for a distribution company. Therefore, the minimization of active power losses is one of the most common and important objective functions in OPF studies used by distribution system operators. Considering different (reduced) scenarios for PV generation and load profiles with their respective probabilities, the objective function for ORPD can be formulated as a minimization of the expected daily energy loss as follows:

$$Fobj1 = \min \left[ \sum_{\xi=1}^{\Xi} W_{loss}^{\xi} p(\xi) \right] \tag{19}$$

$$W_{loss}^{\xi} = \sum_{t=1}^T \sum_{\substack{i=1 \\ \phi \in a, b, c}}^{NB} R_{i,\phi} \left( I_{i,\phi}^{\xi}(t) \right)^2 \tag{20}$$

where  $W_{loss}^{\xi}$  is the total energy loss in scenario  $\xi$ ,  $NB$  is the number of branches in the DN,  $R_{i,\phi}$  is the resistance of branch  $i$  in phase  $\phi$ , and  $I_{i,\phi}^{\xi}$  is the current magnitude through the  $i$ th branch in phase  $\phi$  for scenario  $\xi$ .

#### 3.1.2. Voltage Unbalance Minimization

High penetration of single-phase PV systems and relative variations in per-phase loading lead to an increase in voltage imbalance in distribution networks. It is well known that significant voltage unbalance may lead to higher network losses, increased heating of network components such as transformers, and costly damage or derating of three-phase motors [24]. In this paper, the phase voltage unbalance rate (PVUR) is used as the voltage unbalance metric. The PVUR is calculated at each three-phase bus using the line-to-ground voltage magnitudes ( $V_a$ ,  $V_b$ , and  $V_c$ ) [24]:

$$PVUR(\%) = \frac{\Delta V_p^{\max}}{V_p^{avg}} \cdot 100, \tag{21}$$

where  $V_p^{avg} = \frac{V_a + V_b + V_c}{3}$ ,

$$\Delta V_p^{\max} = \max \left\{ \left| V_a - V_p^{avg} \right|, \left| V_b - V_p^{avg} \right|, \left| V_c - V_p^{avg} \right| \right\}$$

According to IEEE standard 141-1993 [25] the maximum value of PVUR must not exceed 2% for distribution networks. To ensure that the PVUR value at any three-phase bus does not exceed this limit, the minimization of the expected maximum of PVUR in the DN can be defined as an objective function:

$$Fobj2 = \min \left[ \sum_{\xi=1}^{\Xi} PVUR_{\max}^{\xi} p(\xi) \right] \tag{22}$$

where  $PVUR_{\max}^{\xi}$  is the maximum value of the PVUR in the DN for scenario  $\xi$ .

### 3.2. Constraints

#### 3.2.1. Equality Constraints

The equality constraints for the ORPD problem are typical non-linear power flow equations for three-phase unbalanced DNs [26,27].

#### 3.2.2. Inequality Constraints

There are two types of inequality constraints: functional operational constraints, such as slack bus active power limits (23), load bus voltage limits (24), and branch flow limits (25); and feasibility region constraints defined by inverter reactive power limits (26) and slack bus voltage limits (27).

$$P_{grid,min}^\phi \leq P_{grid}^\phi(t) \leq P_{grid,max}^\phi \tag{23}$$

$$V_{i,min}^\phi \leq V_i^\phi(t) \leq V_{i,max}^\phi, \quad i = 1, \dots, NL \tag{24}$$

$$S_i^\phi(t) \leq S_{i,max}^\phi, \quad i = 1, \dots, NB \tag{25}$$

$$-\sqrt{\left(S_{in,i}^\phi\right)^2 - \left(P_{in,i}^\phi(t)\right)^2} \leq Q_{in,i}^\phi(t) \leq \sqrt{\left(S_{in,i}^\phi\right)^2 - \left(P_{in,i}^\phi(t)\right)^2} \tag{26}$$

$$V_{0,min}^\phi \leq V_0^\phi(t) \leq V_{0,max}^\phi \tag{27}$$

where  $P_{grid}^\phi(t)$  is the active power from/to the source grid at time  $t$  in phase  $\phi$ ;  $P_{grid,min}^\phi$  and  $P_{grid,max}^\phi$  are the minimum and maximum power from/to the source grid, respectively;  $V_i^\phi(t)$  is the voltage magnitude at load bus  $i$  in phase  $\phi$ ;  $V_{i,min}^\phi$  and  $V_{i,max}^\phi$  minimum and maximum limits of the voltage magnitude at load buses, respectively;  $S_i^\phi(t)$  and  $S_{i,max}^\phi$  are the apparent power value and maximum apparent power value of the  $i$ th branch in phase  $\phi$ , respectively;  $Q_{in,i}^\phi$  is the reactive power injection of the inverter connected to phase  $\phi$  at the  $i$ th bus;  $S_{in,i}^\phi$  and  $P_{in,i}^\phi(t)$  are the maximum (rated) apparent power and the active power at time  $t$  of the PV (or BESS) inverter connected to phase  $\phi$  at the  $i$ th bus, respectively; and  $V_0^\phi(t)$ ,  $V_{0,min}^\phi$ , and  $V_{0,max}^\phi$  are the value, minimum, and maximum limits of the voltage magnitude at the slack bus in phase  $\phi$ , respectively.

## 4. Solution Method

The hybrid PSOS-CGSA algorithm introduced in [27] was applied to effectively solve the above defined optimal active/reactive power dispatch. This is a metaheuristic population-based optimization algorithm constructed by the hybridization of particle swarm optimization with sigmoid-based acceleration coefficients (PSOS) [28] and the chaotic gravitational search algorithm (CGSA) [29]. Its performance in terms of simplicity, efficiency, and robustness has been demonstrated in solving various complex optimization problems, such as distribution system state estimation [27], dynamic economic dispatch [30], and optimal power flow in DNs [13].

### 4.1. Application of PSOS-CGSA for Active Power Dispatch

In the optimal active power dispatch problem presented in Section 2, the objective function is defined by Equation (10). The control variables are coefficients  $a_\phi(t)$ , which define the power of the BESS according to (8). Therefore, a search agent can be written as:

$$\mathbf{x}_i(t) = [a_{a,i}(t), a_{b,i}(t), a_{c,i}(t)] \quad i = 1, \dots, N \tag{28}$$

where  $N$  is the total number of search agents (population size), and  $a_{\phi,i}(t)$  is the value of control variable  $a$  within search agent  $i$  for phase  $\phi$  at iteration  $t$ .



A summary of the algorithm proposed to solve the active power dispatch is represented by the flowchart in Figure 3.

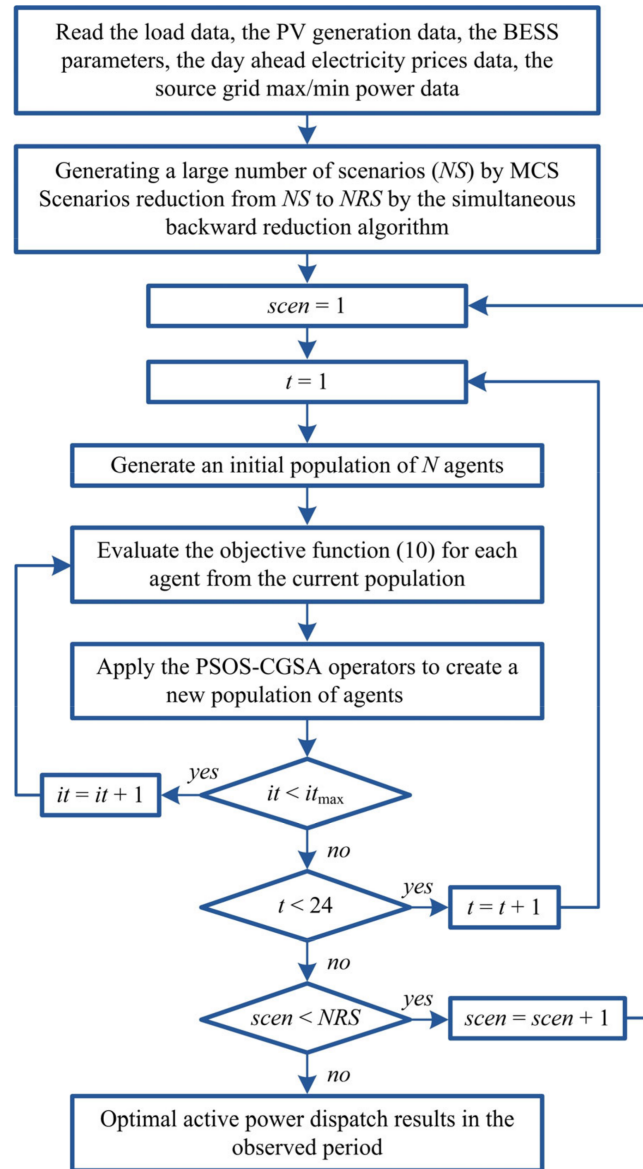


**Figure 3.** Flowchart for the active power dispatch using PSOS-CGSA.

#### 4.2. Application of PSOS-CGSA for Reactive Power Dispatch

The vector of control variables in the problem of ORPD consists of the reactive powers of the PV and BESS inverters and the slack bus voltage magnitudes and can be expressed as follows:

$$\mathbf{x}_i(t) = [Q_{i,1}^\phi(t), \dots, Q_{i,j}^\phi(t), \dots, Q_{i,N_i}^\phi(t), V_0^\phi(t)] \quad i = 1, \dots, N \quad (29)$$

where  $Q_{i,j}^\phi$  is the reactive power of the inverter at the  $j$ th bus in phase  $\phi$ ,  $N_i$  is the total number of buses in which inverters are connected, and  $V_0^\phi$  is the voltage magnitude at the root bus of phase  $\phi \in (a, b, c)$ .

The application of PSOS-CGSA in solving the problem of optimal reactive power dispatch is presented in the flowchart in Figure 4.

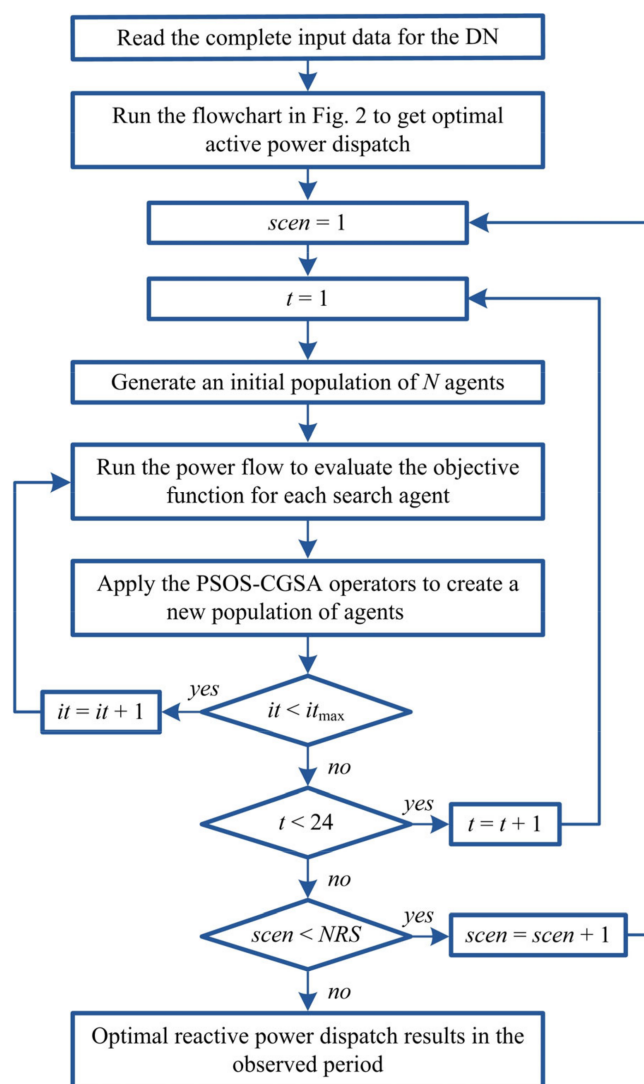


Figure 4. Flowchart for the reactive power dispatch using PSOS-CGSA.

## 5. Simulation Results

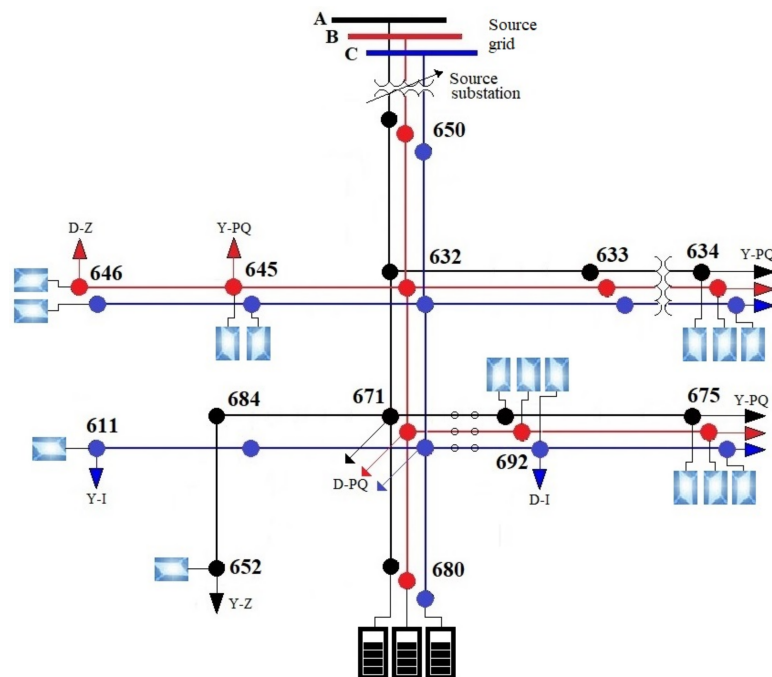
The proposed approach for the day-ahead optimal dispatching of active and reactive powers was simulated on a modified IEEE 13-bus feeder [31]. In the modified IEEE 13-bus feeder, the single-phase PV sources are connected to buses 634, 645, 646, 611, 675, 692, and 652, as shown in Figure 5. Single-phase PV sources, each with the same rated power of 250 kW, are connected to the grid via single-phase inverters. Single-phase BESSs, each with a rated power of 0.9 MW and a capacity of 3.6 MWh, are connected at bus 680 in all three phases via single-phase converters with rated apparent power of 1.1 of the rated power of the batteries. Data on PV and BESS parameters are given in Tables 1 and 2, respectively.

Table 1. Parameters of PV units.

$P_{pvn}$ (kW)	$S_{stc}$ (kW/m <sup>2</sup> )	$R_c$ (kW/m <sup>2</sup> )
250	1	0.12

Table 2. Parameters of BESS.

$P_{bat,chmax}$ (MW)	$P_{bat,dchmax}$ (MW)	$SoC_{max}$ (%)	$SoC_{min}$ (%)	$\eta_{ch} = \eta_{dch}$	$c_{bat}$ (EUR/MWh)
0.9	0.9	80	20	1	10



**Figure 5.** Single-line diagram of the modified IEEE 13-bus test system.

The daily load profile is represented by the mean hourly values shown in Table 3, with a standard deviation of 10%. The daily solar irradiance profile used in the simulation is represented by the mean hourly values and standard deviations given in Table 4. The day-ahead electricity price (EP) data used are shown in Table 5. The maximum value is estimated according to the electricity price for Serbia on the spot market in January–February 2023.

**Table 3.** Load profile data.

Hour	$\mu_L$ (p.u.)	Hour	$\mu_L$ (p.u.)	Hour	$\mu_L$ (p.u.)
1	0.1591	9	0.5644	17	0.6715
2	0.2045	10	0.5372	18	1.0000
3	0.1948	11	0.6026	19	0.9310
4	0.1858	12	0.5496	20	0.7588
5	0.1963	13	0.4893	21	0.8244
6	0.1866	14	0.4847	22	0.9924
7	0.3154	15	0.4493	23	0.7869
8	0.5499	16	0.4390	24	0.5222

**Table 4.** Solar irradiance data.

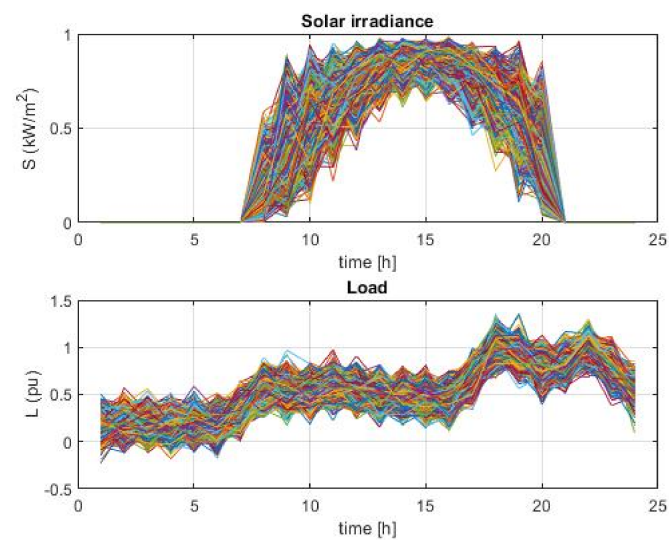
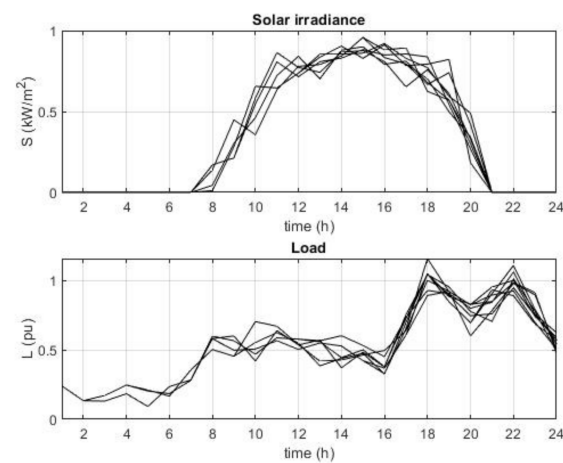
Hour	$\mu_S$ (W/m <sup>2</sup> )	$\sigma_S$ (W/m <sup>2</sup> )
8	158	120
9	386	248
10	538	277
11	669	261
12	748	242
13	819	221
14	862	207
15	870	197
16	853	205
17	779	237
18	700	258
19	572	263
20	357	206

**Table 5.** Electricity price data.

Hour	$c_g$ (EUR/MWh)	Hour	$c_g$ (EUR/MWh)	Hour	$c_g$ (EUR/MWh)
1	67.59	9	83.53	17	82.02
2	65.31	10	81.26	18	82.77
3	52.40	11	72.14	19	85.05
4	45.56	12	68.35	20	88.85
5	50.12	13	65.31	21	101.00
6	59.23	14	65.00	22	91.13
7	71.38	15	68.04	23	80.50
8	82.02	16	72.90	24	73.66

### 5.1. OAPD Results

As explained in Section 2, using MCS, there are 2000 solar irradiance and load scenarios generated, as shown in Figure 6. By applying the simultaneous backward reduction technique, these 2000 scenarios were reduced to the 10 scenarios shown in Figure 7.

**Figure 6.** Scenarios generated by MCS.**Figure 7.** Reduced scenarios of solar irradiance and load.

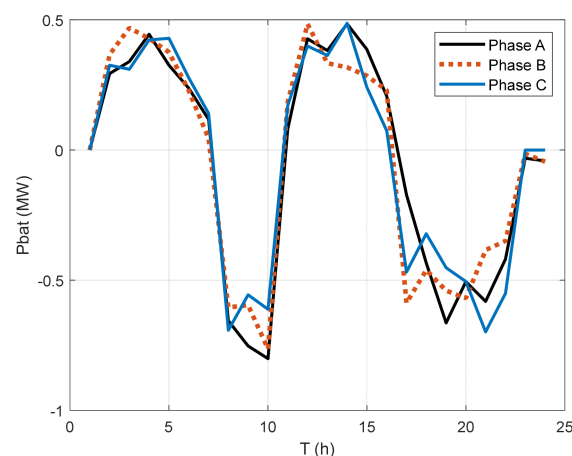
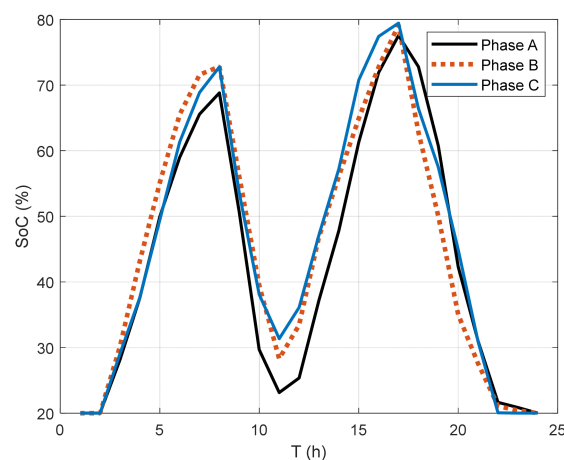
By applying the proposed approach for the optimal active power dispatch, the expected total operating costs of each scenario were determined; the results are shown in Table 6.

**Table 6.** Expected costs.

Scenario	Probability	Cost (€)
1	0.0420	440.22
2	0.0760	590.36
3	0.0565	483.70
4	0.0760	552.52
5	0.0580	361.21
6	0.1100	462.06
7	0.2250	416.95
8	0.1265	<b>339.61</b>
9	0.1205	524.65
10	0.1095	444.86
<b>Expected</b>		<b>453.16</b>

Bold indicates the best results.

The optimal value of the expected daily cost for electricity is EUR 453.16. According to (10), this value is obtained as the sum of the costs in each reduced scenario multiplied by the corresponding probability. In view of this, the expected day-ahead charging/discharging schedule of the BESS was obtained as shown in Figures 8 and 9.

**Figure 8.** Expected battery power during the day.**Figure 9.** Expected battery SoC during the day.

For comparison, Figure 10 shows the daily costs for electricity in the following cases: (i) without a BESS integrated into the DN (base case), (ii) with a BESS in the DN applying the charge/discharge schedule approach presented in [13], and (iii) with the BESS in the

DN using the proposed OAPD algorithm. The results in Figure 10 clearly indicate that the proposed PSOS-CGSA-based approach for OAPD leads to a large reduction in costs for electricity compared to the base case and the approach for OAPD in [13].

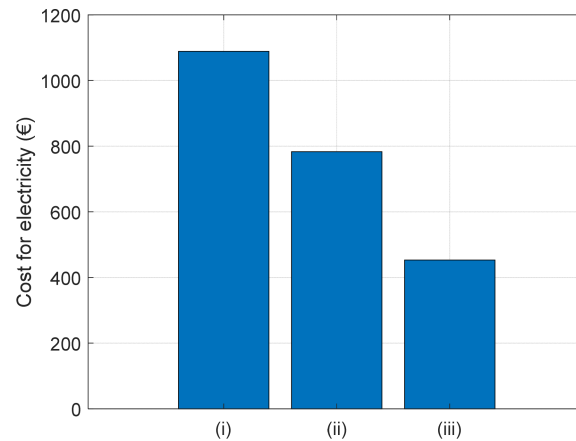


**Figure 10.** Comparison of expected daily costs for electricity: (i) without BESS, (ii) with the BESS using approach in [13], and (iii) with the BESS using the proposed OAPD algorithm.

### 5.2. ORPD Results

Here, the optimal values of 21 control variables should be determined, as follows:

$$\mathbf{x} = \left[ \begin{array}{cccccccccccccccccccc} Q_{634}^a, Q_{634}^b, Q_{634}^c, Q_{645}^b, Q_{645}^c, Q_{646}^b, Q_{646}^c, Q_{692}^a, Q_{692}^b, Q_{692}^c, \dots \\ Q_{675}^a, Q_{675}^b, Q_{675}^c, Q_{611}^c, Q_{652}^a, Q_{680}^a, Q_{680}^b, Q_{680}^c, V_{650}^a, V_{650}^b, V_{650}^c \end{array} \right]$$

The simulation studies were performed for the following two test cases:

Case 1: Minimization of the active power losses (Fobj1);

Case 2: Minimization of the phase voltage unbalance rate (Fobj2).

The voltages at the load buses must be within the range of [0.94–1.06] (p.u.). The voltage of the root bus ( $V_0$ ) can be changed in the range of [0.9–1.1] (p.u.), while the limits of the reactive power of the converter are variable, according to (26).

The results are given in Tables 7 and 8. In the base case, the PV sources and BESS operate with unity power factor, and the root bus voltage is equal to 1 p.u. Tables 7 and 8 show the expected values of total active energy losses ( $W_{loss}$ ) and maximum values of the phase voltage unbalance rate ( $PVUR_{max}$ ), respectively, for all ten reduced scenarios.

**Table 7.** ORPD results for  $W_{loss}$ .

Scenario	Probability	$W_{loss}$ (kWh)		
		Base	Case 1	Case 2
1	0.0420	969.62	725.76	849.90
2	0.0760	931.60	730.77	859.22
3	0.0565	878.93	681.53	813.92
4	0.0760	931.63	726.75	879.11
5	0.0580	973.22	761.71	882.67
6	0.1100	1016.80	805.72	951.66
7	0.2250	937.08	724.04	873.22
8	0.1265	990.97	776.68	919.96
9	0.1205	804.23	<b>616.91</b>	759.31
10	0.1095	977.61	772.15	905.42
<b>Expected</b>		940.44	<b>732.62</b>	873.16

Bold indicates the best results.

**Table 8.** ORPD results for  $PVUR_{max}$ .

Scenario	Probability	$PVUR_{max}$ (%)		
		Base	Case 1	Case 2
1	0.0420	12.54	7.70	<b>1.14</b>
2	0.0760	10.45	6.46	2.93
3	0.0565	8.42	7.43	2.05
4	0.0760	8.97	7.32	1.51
5	0.0580	11.91	6.46	2.75
6	0.1100	10.01	7.85	2.67
7	0.2250	8.34	6.46	1.71
8	0.1265	8.06	6.83	1.16
9	0.1205	6.46	7.58	1.46
10	0.1095	10.55	6.43	2.29
<b>Expected</b>		9.10	6.96	<b>1.91</b>

Bold indicates the best results.

Applying the proposed procedure for ORPD achieves a reduction in expected energy losses of 22% compared to the base case, while the expected value of the maximum  $PVUR$  drops from 9.1% to 1.91%. There are significant energy savings, and it is ensured that the  $PVUR$  index level is below the maximum limit of 2% for all three-phase buses in the DN.

Based on the results shown in Tables 7 and 8, it can be seen that in the case of the minimization of active energy losses ( $Fobj1$ ), the best scenario is 9, and in the case of the minimization of the voltage unbalance ( $Fobj2$ ), the best scenario is scenario 1. Figures 11 and 12 show the optimal values of the control variables for these best scenarios.

The voltage profiles at bus 671 for the best scenario in Case 1 and the best scenario in Case 2 are shown in Figures 13 and 14, respectively.

In Case 1, ORPD reduces the active energy losses compared to the base case, while the voltages are within the permissible limits, as shown in Figure 13. The phase voltage magnitudes are much closer to each other in Case 2 (Figure 14) than in Case 1 (Figure 13). Clearly, this is as a consequence of the  $PVUR$  minimization in Case 2.

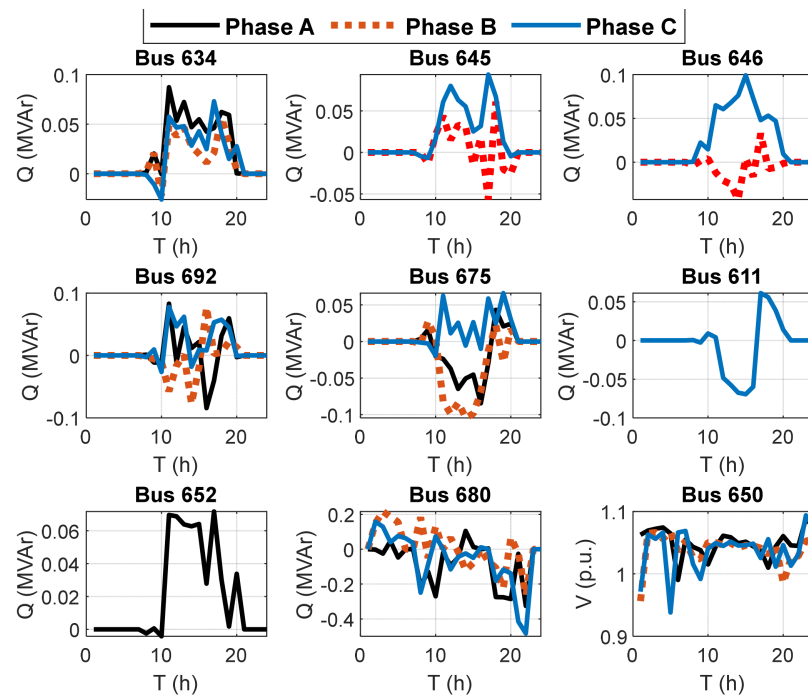


**Figure 11.** Optimal values of control variables for the best scenario (9) in Case 1.

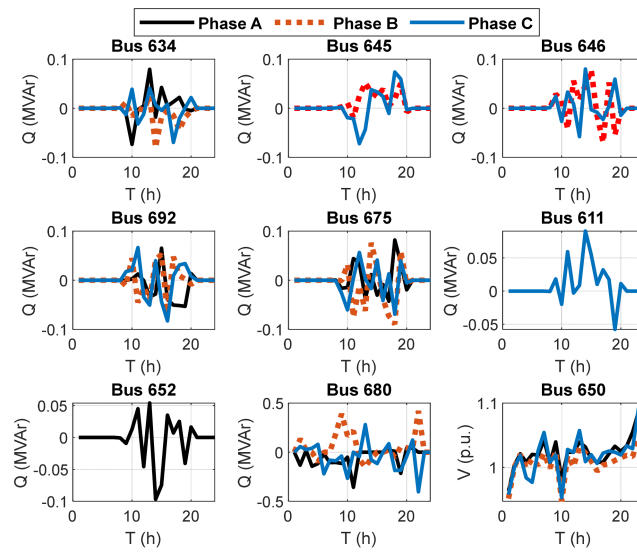


Figure 12. Optimal values of control variables for the best scenario (1) in Case 2.

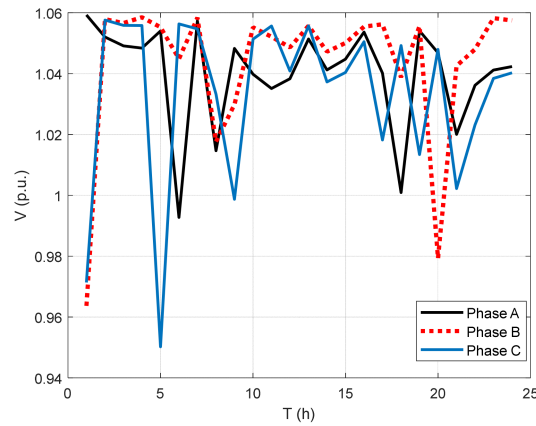


Figure 13. Voltage profile at bus 671 in Case 1.

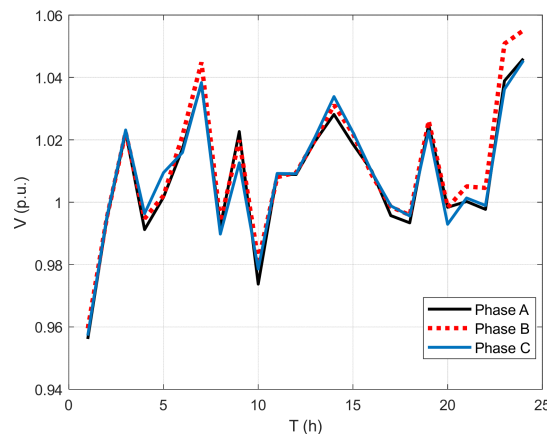


Figure 14. Voltage profile at bus 671 in Case 2.

### 5.3. Evaluation of PSOS-CGSA

The efficiency of the proposed solution algorithm (PSOS-CGSA) [27,30] was confirmed by a comparison with well-established metaheuristic algorithms genetic algorithm (GA) [32], particle swarm optimization (PSO) [33], and the gravitational search algorithm (GSA) [34]; their recently improved versions, PSOS [28] and CGSA [29], phasor PSO



(PPSO) [35], hybrid PSO and GSA (PSO-GSA) [36], and hybrid PPSO and GSA (PPSO-GSA) [2]; and two recently proposed algorithms, namely the arithmetic optimization algorithm (AOA) [37] and the tunicate swarm algorithm (TSA) [38].

Algorithm parameters were adopted based on their default values in the cited references. The population size and maximum iteration number were set as  $N = 50$  and  $it_{max} = 200$  for all case studies. All algorithms were employed to solve the problem of OAPD under the same terms and input data.

The daily costs for electricity obtained for all 10 reduced scenarios are shown in Figure 15. Furthermore, the expected daily costs for electricity obtained using different solution methods are shown in Figure 16. It is clear that the proposed hybrid PSOS-CGSA method finds better solutions for the OAPD problem, i.e., provides lower costs in each of 10 scenarios and the least expected daily cost for electricity compared to other algorithms.

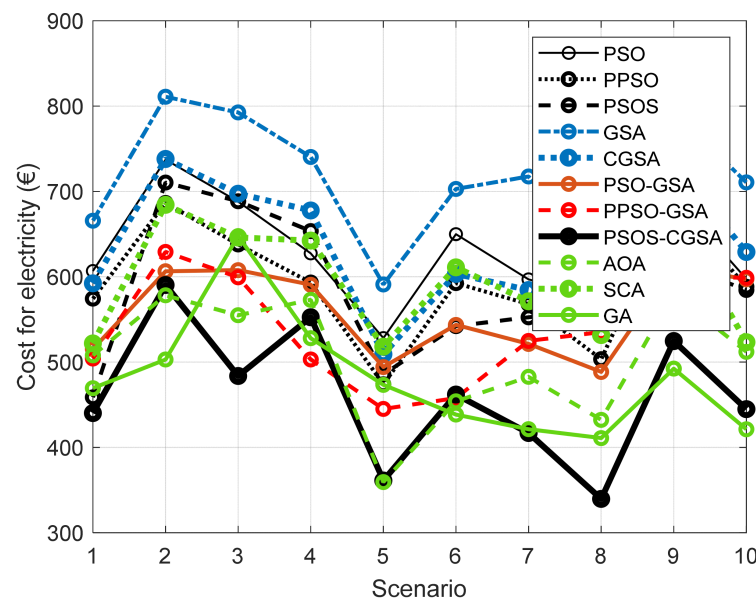


Figure 15. Comparison of solution methods applied for OAPD.

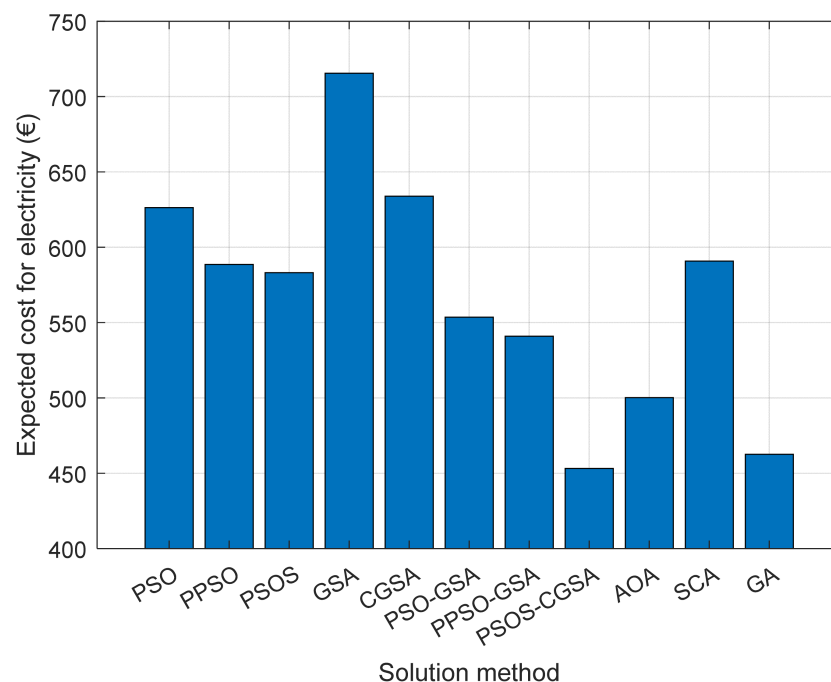


Figure 16. Comparison of expected daily electricity costs obtained by different methods.

## 6. Conclusions

In this paper, a two-stage approach for the dynamic day-ahead optimal active-reactive power dispatch in unbalanced DNs with high penetration of single-phase solar PV systems and BESS was proposed. The simulation results conducted on a modified IEEE 13-bus test system indicate the conclusions that can be summarized as follows:

- The proposed OAPD ensures minimum costs for electricity from the source grid for all scenarios generated by the MSC method and the simultaneous backward reduction algorithm;
- Single-phase PV inverters and BESSs can serve as efficient reactive power management resources;
- The proposed ORPD approach enables the reduction in active power losses in the DN and the reduction in the voltage unbalance on the three-phase load buses below the permitted limit;
- The proposed PSOS-CGSA solution technique provides better solutions for optimal power dispatch problems compared to other well-established metaheuristic algorithms, such as GA, PSO, GSA, and modified and hybrid versions of PSO and GSA.

The proposed methodology performed very well for the assumptions and limitations applied in this study. In future work, we plan to relax two of the most important assumptions, namely inclusion of operating costs of PV generation in the OAPD model and consideration the ORPD model regarding other power quality parameters, such as harmonic distortion. This will be accomplished by extending the objective functions for the OAPD model and implementing an algorithm for harmonic power flows in the ORPD model, taking into account non-linear loads and corresponding constraints.

**Author Contributions:** J.R.: conceptualization, methodology, and writing—original draft preparation; A.K.: writing—review and supervision; M.G., M.M. and J.Ž.: investigation, software, validation, and visualization. All authors have read and agreed to the published version of the manuscript.

**Funding:** This research was funded by the Government of the Republic of Serbia, grant number TR 33046.

**Data Availability Statement:** The data presented in this study are available on request from the corresponding author.

**Conflicts of Interest:** The authors declare no conflict of interest.

## References

1. IRENA. *Renewable Power Generation Costs in 2020*; International Renewable Energy Agency: Abu Dhabi, United Arab Emirates, 2021.
2. Radosavljević, J.; Arsić, N.; Milovanović, M.; Ktena, A. Optimal placement and sizing of renewable distributed generation using hybrid metaheuristic algorithm. *J. Mod. Power Syst. Clean Energy* **2020**, *8*, 499–510. [[CrossRef](#)]
3. Luo, X.; Wang, J.; Donner, M.; Clarke, J. Overview of current development in electrical energy storage technologies and application potential in power system operation. *Appl. Energy* **2015**, *137*, 511–536. [[CrossRef](#)]
4. Thango, B.A.; Bokoro, P.N. Battery Energy Storage for Photovoltaic Application in South Africa: A Review. *Energies* **2022**, *15*, 5962. [[CrossRef](#)]
5. Gabash, A. Active-reactive optimal power flow in distribution networks with embedded generation and battery storage. *IEEE Trans. Power Syst.* **2012**, *27*, 2026–2035. [[CrossRef](#)]
6. Mehrjerdi, H.; Hemmati, R. Modeling and optimal scheduling of battery energy storage systems in electric power distribution networks. *J. Clean. Prod.* **2019**, *234*, 810–821. [[CrossRef](#)]
7. Adewuyi, O.B.; Shigenobu, R.; Ooya, K.; Senjyu, T. Static voltage stability improvement with battery energy storage considering optimal control of active and reactive power injection. *Electr. Power Syst. Res.* **2019**, *172*, 303–312. [[CrossRef](#)]
8. Li, X.; Ma, R.; Gan, W.; Yan, S. Optimal dispatch for battery energy storage station in distribution network considering voltage distribution improvement and peak load shifting. *J. Mod. Power Syst. Clean Energy* **2022**, *10*, 131–139. [[CrossRef](#)]
9. Milošević, D.; Đurišić, Ž. Technique for stability enhancement of microgrids during unsymmetrical disturbances using nattery connected by single-phase converters. *IET Renew. Power Gener.* **2020**, *14*, 1529–1540. [[CrossRef](#)]
10. Watson, J.D.; Watson, N.R.; Lestas, I. Optimized dispatch of energy storage systems in unbalanced distribution networks. *IEEE Trans. Sustain. Energy* **2018**, *9*, 639–650. [[CrossRef](#)]
11. Das, K.; Grapponon, A.L.T.P.; Sorensen, P.E.; Hansen, A.D. Optimal battery operation for revenue maximization of wind-storage hybrid power plant. *Electr. Power Syst. Res.* **2020**, *188*, 106–631. [[CrossRef](#)]

12. Prudhviraaj, D.; Kiran, P.B.S.; Pindoriya, N.M. Stochastic energy management of microgrid with nodal price. *J. Mod. Power Syst. Clean Energy* **2020**, *8*, 102–110. [[CrossRef](#)]
13. Radosavljević, J.; Milovanović, M.; Arsić, N.; Jovanović, A.; Perović, B.; Vukašinović, J. Optimal power dispatch in distribution networks with PV generation and battery storage. In Proceedings of the IX International Conference on Electrical, Electronic and Computing Engineering IcETRAN 2022, Novi Pazar, Serbia, 6–9 June 2022.
14. Giuntoli, M.; Subasic, M.; Schmitt, S. Control of distribution grids with storage using nested Benders' decomposition. *Electr. Power Syst. Res.* **2021**, *190*, 106663. [[CrossRef](#)]
15. Khan, H.A.; Zuhaim, M.; Rihan, M. Voltage fluctuation mitigation with coordinated OLTC and energy storage control in high PV penetrating distribution network. *Electr. Power Syst. Res.* **2022**, *208*, 107924. [[CrossRef](#)]
16. Radosavljević, J. Voltage regulation in LV distribution networks with PV generation and battery storage. *J. Electr. Eng.* **2021**, *72*, 356–365. [[CrossRef](#)]
17. Udawalpola, R.; Masuta, T.; Yoshioka, T.; Takahashi, K.; Ohtake, H. Reduction of Power Imbalances Using Battery Energy Storage System in a Bulk Power System with Extremely Large Photovoltaics Interactions. *Energies* **2021**, *14*, 522. [[CrossRef](#)]
18. Biswas, P.P.; Suganthan, P.N.; Amaratunga, G.A.J. Optimal power flow solutions incorporating stochastic wind and solar power. *Energy Convers. Manag.* **2017**, *148*, 1194–1207. [[CrossRef](#)]
19. Gröwe-Kuska, N.; Heitsch, H.; Römisch, W. Scenario reduction and scenario tree construction for power management problems. In Proceedings of the 2003 IEEE Bologna PowerTech—Conference Proceedings, Bologna, Italy, 23–26 June 2003; Volume 3, pp. 152–158.
20. LNesp. Scenred. GitHub. Available online: <https://github.com/supsi-dacd-isaac/scenred> (accessed on 22 February 2023).
21. Maheshwari, A.; Sood, Y.R.; Jaiswal, S. Flow direction algorithm-based optimal power flow analysis in the presence of stochastic renewable energy sources. *Electr. Power Syst. Res.* **2023**, *216*, 109087. [[CrossRef](#)]
22. Ali, A.; Mahmoud, K.; Raisz, D.; Lehtonen, M. Probabilistic approach for hosting high PV penetration in distribution systems via optimal oversized inverter with watt-var functions. *IEEE Syst. J.* **2021**, *15*, 684–693. [[CrossRef](#)]
23. Xavier, L.S.; Amorim, W.C.S.; Cupertino, A.F.; Mendes, V.F.; Boaventura, W.C.; Pereira, H.A. Power converters for battery energystorage systems connected to mediumvoltage systems: A comprehensive review. *BMC Energy* **2019**, *1*, 7. [[CrossRef](#)]
24. Girigoudar, K.; Roald, L.A. On the impact of different voltage unbalance metrics in distribution system optimization. *Electr. Power Syst. Res.* **2019**, *189*, 106656. [[CrossRef](#)]
25. *IEEE Standard 141–1993*; Recommended Practice for Electric Power Distribution for Industrial Plants. IEEE: New York, NY, USA, 1994; pp. 1–768.
26. Khushalani, S.; Solanki, K.M.; Shulz, N.N. Development of three-phase unbalanced power flow using PV and PQ models for distributed generation and study of the impact of DG models. *IEEE Trans. Power Syst.* **2007**, *22*, 1019–1025. [[CrossRef](#)]
27. Ullah, Z.; Elkadeem, M.R.; Wang, S.; Radosavljević, J. A Novel PSOS-CGSA Method for State Estimation in Unbalanced DG-integrated Distribution Systems. *IEEE Access* **2020**, *8*, 113219–113229. [[CrossRef](#)]
28. Tian, D.; Zhao, X.; Shi, Z. Chaotic particle swarm optimization with sigmoid-based acceleration coefficients for numerical function optimization. *Swarm Evol. Comput.* **2019**, *51*, 100573. [[CrossRef](#)]
29. Mirjalili, S.; Gandomi, A.H. Chaotic gravitational constants for the gravitational search algorithm. *Appl. Soft Comput.* **2017**, *53*, 407–419. [[CrossRef](#)]
30. Radosavljević, J.; Arsić, N.; Štatkić, S. Dynamic Economic Dispatch Considering WT and PV Generation using Hybrid PSOS-CGSA Algorithm. In Proceedings of the 20th International Symposium INFOTEH-JAHORINA (INFOTEH), East Sarajevo, Bosnia and Herzegovina, 17–19 March 2021; pp. 1–6.
31. IEEE PES Test Feeder. Available online: <https://cmt.ee.org/pes-testfeeders/resources/> (accessed on 18 February 2023).
32. Yarpiz. Available online: <https://yarpiz.com/23/ypea101-genetic-algorithms> (accessed on 2 May 2023).
33. Kennedy, J.; Eberhart, R.C. Particle swarm optimization. In Proceedings of the IEEE International Conference on Neural Networks, Perth, Australia, 27 November–1 December 1995; pp. 1942–1948.
34. Rashedi, E.; Nezamabadi-pour, H.; Saryazdi, S. GSA: A gravitational search algorithm. *Inf. Sci.* **2009**, *179*, 2232–2248. [[CrossRef](#)]
35. Ghasemi, M.; Akbari, E.; Rahimnejad, A.; Razavi, S.E.; Ghavidel, S.; Li, L. Phasor particle swarm optimization: A simple and efficient variant of PSO. *Soft Comput.* **2019**, *19*, 9701–9718. [[CrossRef](#)]
36. Mirjalili, S.; Hashim, S.Z.M. A new hybrid PSOGSA algorithm for function optimization. In Proceedings of the IEEE International Conference on Computer and Information Application, Tianjin, China, 3–5 December 2010; pp. 374–377.
37. Abualgah, L.; Diabat, A.; Mirjalili, S.; Abd Elaziz, M.; Gandomi, A.H. The Arithmetic Optimization Algorithm. *Comput. Methods Appl. Mech. Eng.* **2021**, *376*, 113609. [[CrossRef](#)]
38. Kaur, S.; Awasthi, L.K.; Sangal, A.L.; Dhiman, G. Tunicate Swarm Algorithm: A new bio-inspired based metaheuristic paradigm for global optimization. *Eng. Appl. Artif. Intell.* **2020**, *90*, 103541. [[CrossRef](#)]

**Disclaimer/Publisher's Note:** The statements, opinions and data contained in all publications are solely those of the individual author(s) and contributor(s) and not of MDPI and/or the editor(s). MDPI and/or the editor(s) disclaim responsibility for any injury to people or property resulting from any ideas, methods, instructions or products referred to in the content.